

X-ray emission line gas in the LINER galaxy M81 *

M.J. Page¹, A.A. Breeveld¹, R. Soria¹, K. Wu¹, G. Branduardi-Raymont¹, K.O. Mason¹, R.L.C. Starling¹,
and S. Zane¹

¹ Mullard Space Science Laboratory, University College London, Holmbury St Mary, Dorking, Surrey, RH5 6NT, UK

Received 23-04-02; accepted 23-12-02

Abstract. We present the soft X-ray spectrum of the LINER galaxy M81 derived from a long observation with the *XMM-Newton* RGS. The spectrum is dominated by continuum emission from the active nucleus, but also contains emission lines from Fe L, and H-like and He-like N, O, and Ne. The emission lines are significantly broader than the RGS point-source spectral resolution; in the cross dispersion direction the emission lines are detected adjacent to, as well as coincident with, the active nucleus. This implies that they originate in a region of a few arc-minutes spatial extent (1 arc-minute \sim 1 kpc in M81). The flux ratios of the OVII triplet suggest that collisional processes are responsible for the line emission. A good fit to the whole RGS spectrum is obtained using a model consisting of an absorbed power law from the active nucleus and a 3 temperature optically thin thermal plasma. Two of the thermal plasma components have temperatures of 0.18 ± 0.04 keV and 0.64 ± 0.04 keV, characteristic of the hot interstellar medium produced by supernovae; the combined luminosity of the plasma at these two temperatures accounts for all the unresolved bulge X-ray emission seen in the *Chandra* observation by Tennant et al. (2001). The third component has a higher temperature ($1.7_{-0.5}^{+2.1}$ keV), and we argue that this, along with some of the 0.64 keV emission, comes from X-ray binaries in the bulge of M81.

Key words. X-rays: galaxies – ISM: supernova remnants – Galaxies: individual: M81 – Galaxies: active

1. Introduction

M81 is an Sab spiral galaxy hosting a low luminosity Seyfert nucleus which shows the characteristics of a “low ionization nuclear emission-line region” (LINER, Heckman 1980). LINERs make up a significant fraction of all galaxies (between 1/5 and 1/3; Ho et al. 1997), and because M81 is the nearest LINER it is an important target with which to investigate the X-ray emission from such objects.

M81 has been the subject of a number of X-ray studies. It was first observed with *Einstein* (Elvis & van Speybroeck 1982, Fabbiano 1988) which resolved several discrete sources in M81, the brightest of which was associated with the active nucleus. An apparently diffuse emission component associated with the bulge of M81, spatially extended over a few arc-minutes was detected first with *ROSAT* (Roberts & Warwick 2000, Immler & Wang 2001) and confirmed using *Chandra* data (Tennant et al. 2001). Low resolution X-ray spectroscopy of M81 from the *Einstein* MPC and IPC suggested that the nuclear X-

ray source has an intrinsic column density of $> 10^{21} \text{cm}^{-2}$ (Elvis & van Speybroeck 1982, Fabbiano 1988). Later, spectra from *ROSAT* (Immler & Wang 2001), *BBXRT* (Petre et al. 1993), *ASCA* (Ishisaki et al. 1996) and *BeppoSAX* (Pellegrini et al. 2000) indicated the presence of a soft (< 1 keV) thermal component in addition to an absorbed power law component ($\Gamma \sim 2$) from the nucleus. In this paper we present the soft X-ray spectrum of M81 at much higher resolution, from an observation with the *XMM-Newton* reflection grating spectrometer (RGS, den Herder et al. 2001).

2. RGS data reduction and spectral analysis

2.1. Data reduction

M81 was observed by *XMM-Newton* on the 22nd and 23rd April 2001 for a total of 138 ks. The RGS data were reduced using the *XMM-Newton* science analysis system (SAS) public release version 5.2 and the latest calibration files (as of December 2001). The source spectrum was extracted from a region centred on the nucleus, enclosing 90% of the point spread function in the cross dispersion direction, while first and second order selection was performed so as to include 93% of the expected CCD pulse height distribution of the source photons. Background re-

Send offprint requests to: M.J.Page (mjp@mssl.ucl.ac.uk)

* Based on observations obtained with XMM-Newton, an ESA science mission with instruments and contributions directly funded by ESA Member States and the USA (NASA)

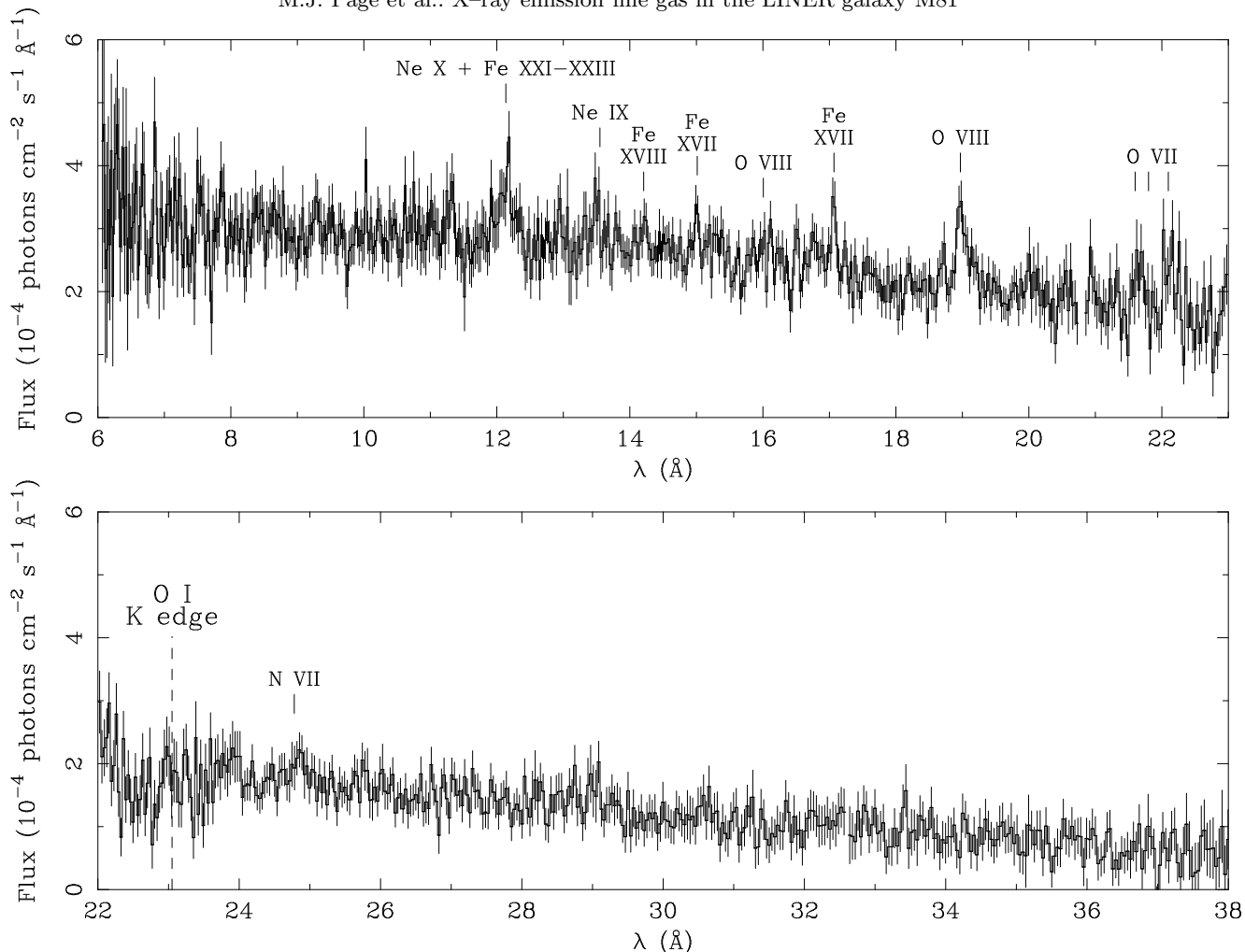


Fig. 1. The combined RGS spectrum with some prominent emission lines marked.

gions were selected in the cross-dispersion direction so as to exclude 99% of the nuclear point spread function; identical order selection was performed on nuclear and background regions. Instrumental features such as that near the oxygen edge at ~ 23 Å were corrected by dividing the effective area calibration in each response matrix by the model/data ratio from a power law fit to the RGS spectrum of the continuum source Mrk 421 (this correction is $< 10\%$ over most of the wavelength range). First and second order spectra from RGS1 and RGS2 and their corresponding response matrices were resampled to match the RGS1 first order spectrum, combined, and rebinned by a factor of 3 (to ~ 30 mÅ bins) to improve signal to noise ratio before spectral analysis using XSPEC.

2.2. X-ray emission line gas

Fig. 1 shows the RGS spectrum. A number of prominent emission lines from H-like and He-like N, O, and Ne as well as L shell lines from Fe XVII – Fe XXIII are visible above the continuum; these are labelled in Fig. 1, and the most significant lines are listed in Table. 1. The lines are considerably broader than the RGS line spread function

Table 1. Fluxes and equivalent widths of the most significant emission lines in the RGS spectrum. The fluxes have been corrected for Galactic absorption. Errors are quoted at 95% for 1 interesting parameter.

λ (Å)	ion	EW (mÅ)	Flux (10^{-5} photon cm^{-2} s^{-1})
$12.15^{+0.04}_{-0.05}$	Ne X*	61^{+24}_{-26}	$2.0^{+0.8}_{-0.8}$
$13.49^{+0.04}_{-0.04}$	Ne IX**	34^{+22}_{-24}	$1.1^{+0.7}_{-0.8}$
$14.22^{+0.06}_{-0.09}$	Fe XVIII	17^{+13}_{-15}	$0.53^{+0.41}_{-0.47}$
$15.01^{+0.03}_{-0.03}$	Fe XVII	27^{+13}_{-18}	$0.83^{+0.40}_{-0.56}$
$17.06^{+0.02}_{-0.02}$	Fe XVII	48^{+20}_{-22}	$1.4^{+0.6}_{-0.7}$
$18.99^{+0.04}_{-0.03}$	O VIII	118^{+31}_{-32}	$2.5^{+0.6}_{-0.7}$
$21.67^{+0.10}_{-0.10}$	O VII	51^{+48}_{-45}	$1.3^{+1.3}_{-1.2}$
$22.12^{+0.07}_{-0.07}$	O VII	79^{+57}_{-55}	$2.0^{+1.4}_{-1.4}$
$24.86^{+0.07}_{-0.10}$	N VII	49^{+48}_{-34}	$1.1^{+1.1}_{-0.8}$

* blended with emission from Fe XXIII

** blended with emission from Fe XIX-XXI

for a point source (~ 70 mÅ FWHM; den Herder et al. 2001). For example, O VIII Ly α at ~ 19 Å is expected to have relatively little contamination from neighbouring

lines, but a gaussian fit to this line shows that its intrinsic width is inconsistent with $\sigma = 0$ at $> 99\%$. This level of line broadening could occur if the gas is extended over a region of ~ 2 arc-minutes, because the RGS is a slitless dispersive spectrograph and its resolution is degraded for extended objects. Alternatively, the broadening could be due to kinematic motions in the gas, for example if it is associated with the active nucleus.

To distinguish between these alternatives, we have examined the spatial distribution of the emission line gas in the RGS cross dispersion direction by constructing spectra in 40 arc-second wide strips at a range of distances from the nucleus of M81 (for comparison, the cross dispersion region used in Sect. 2.1 varies from ~ 52 arc-seconds wide around 20\AA to ~ 75 arc-seconds wide near the ends of the spectrum). The spectra were binned to 60 m\AA and a background spectrum was constructed from the average of the two most off-axis strips; this was subtracted from all the spectra. The emission-line rich $14\text{-}20\text{ \AA}$ parts of these spectra are shown in Fig. 2. The emission line gas, and in particular O VIII Ly α , is extended over more than an arc-minute implying that the excess broadening of the emission lines is due to their spatial extent, rather than kinematic motions.

We further investigate the nature of the emission line gas using plasma diagnostics from the He-like OVII triplet, as described in Porquet & Dubau (2000). Taking the $21\text{-}23\text{ \AA}$ portion of the RGS spectrum, and assuming an underlying power law continuum ($\Gamma = 2$, see Sect. 2.3), we fitted the OVII lines as 3 gaussians with the relative wavelengths of the resonance (w), intercombination (x+y) and forbidden (z) lines fixed at their theoretical ratios. The best fit has an acceptable $\chi^2/\nu = 56/51$, and is shown superimposed on the $21\text{-}23\text{ \AA}$ RGS spectrum in Fig. 3a. In Fig. 3b we show the confidence contour of the (x+y+z) against w line strength, a diagnostic of the ionization mechanism. The solid line shows the line ratio $G = (x+y+z)/w = 4$. As shown in figure 7 of Porquet & Dubau (2000), plasmas in which photoionization is the dominant ionization mechanism are expected to have ratios to the left of this line (i.e. $G > 4$); this is ruled out at 95% confidence ($\Delta\chi^2 > 4$ for one interesting parameter G) in M81. For plasmas with line ratios to the right of this line, such as that observed in M81, collisional excitation is important and may be the dominant emission mechanism. If the O VII lines arise in a collisionally ionized plasma, the G ratio provides a temperature diagnostic; by comparison with Porquet et al. (2001) we find that the lines arise in a plasma with $kT < 0.26\text{ keV}$ at 90% confidence.

Fig. 3c shows confidence contours of the density diagnostic z against (x+y). The line shown on the plot corresponding to ratio $R = z/(x+y) = 1$ is excluded at $> 95\%$ along with all of parameter space to the right of this line, implying (see Porquet & Dubau 2000 figure 8) that the line emitting plasma has a density of $n_e < 10^{11}\text{ cm}^{-3}$. The best fit has very weak x+y lines relative to z, and consequently lies to the left of the line $R = 3.5$, hence the line

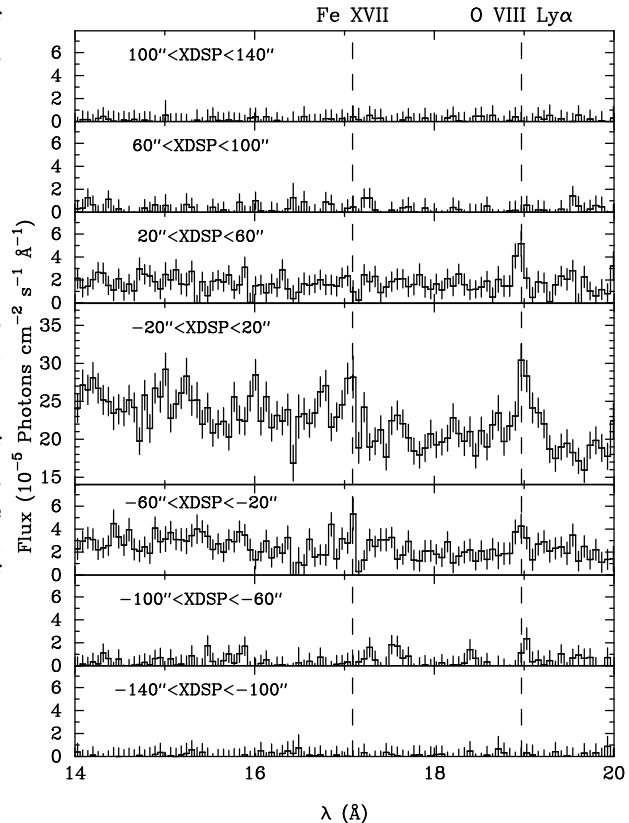


Fig. 2. Spectral cuts labeled with distance from the nucleus in the cross dispersion direction (XDSP) demonstrating that the line emission comes from a spatially extended region. The dashed lines correspond to prominent emission lines from FeXVII and OVIII.

ratio observed in M81 is best reproduced by a low density ($n_e < 10^9\text{ cm}^{-3}$) plasma.

2.3. Modelling the whole RGS spectrum

It is evident from Fig. 1 that the emission lines in the soft X-ray spectrum of M81 are superimposed on a strong continuum source, almost certainly from the active nucleus at the heart of M81. Therefore we began by fitting a power law model with absorption (using the XSPEC model TBabs of Wilms et al. 2000) by the line of sight Galactic column density $N_H = 4.16 \times 10^{20}\text{ cm}^{-2}$ (Dickey & Lockman 1990). The parameters of this fit, and subsequent fits, are given in Table 2. We found that the power law model is a poor fit with $\chi^2/\nu = 1289/993$; the model overpredicts the data at both the high and low wavelength ends of the spectrum, and has too small an O I edge at 23 \AA . We therefore added additional cold absorption, and obtained a much better fit ($\chi^2/\nu = 1085/992$), with an additional $N_H \sim 5 \times 10^{20}\text{ cm}^{-2}$. This additional column density confirms, and is consistent with, previous results (e.g. Pellegrini et al. 2000) that the nucleus of M81 has some intrinsic absorption.

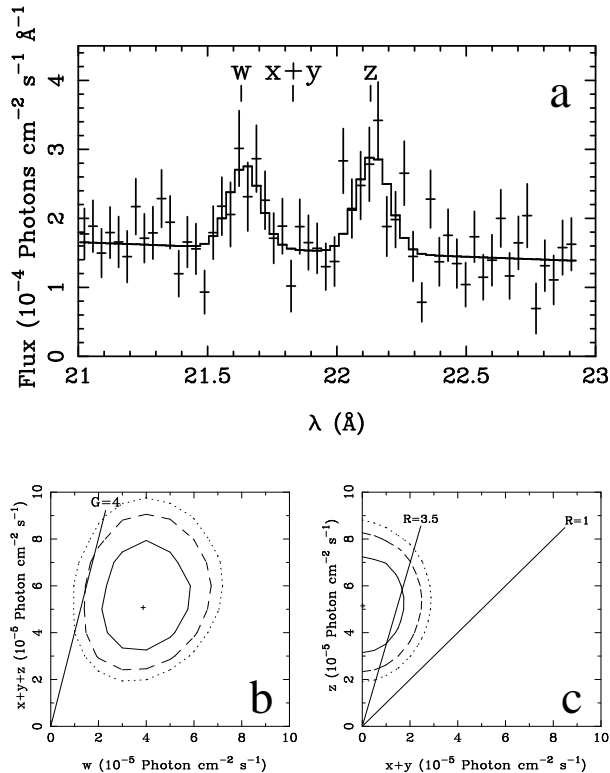


Fig. 3. Panel a. shows the O VII triplet and best fit model. Panel b. shows the 68% (solid), 90% (dashed) and 95% (dotted) confidence contours for the intercombination (x+y) and forbidden (z) line strength against the resonance (w) line strength; photoionization powered lines should have line ratios to the left of the line $G = (x+y+z)/w = 4$. Panel c. shows 68% (solid), 90% (dashed) and 95% (dotted) confidence contours for the forbidden (z) line strength against the intercombination (x+y) line strength; the ratios $R = z/(x+y) = 1$ and $R = 3.5$ correspond to densities of $\sim 10^{11} \text{cm}^{-3}$ and $\sim 10^9 \text{cm}^{-3}$ respectively.

We then attempted to model the emission line component of the spectrum. As shown in Sect. 2.2 the O VII triplet is consistent with an origin in a collisionally ionized gas, and the line emission comes from a region extended over several kpc. We therefore began modelling the emission lines by adding a single-temperature, solar-abundance ‘Mekal’ thermal plasma model to the absorbed power law model. This resulted in a significant improvement in the fit ($\chi^2/\nu = 876/990$) for a plasma temperature of 0.66 ± 0.04 keV.

However, the emission lines are too narrow in this model (the excessive width of the emission lines has already been pointed out in Sect. 2.2), and some emission lines, particularly those from OVII, have much lower intensities in the model than in the observed spectrum (see Fig. 4). We addressed the first of these two problems by adding 2 extra Mekal components, shifted by $\pm 0.5\%$ in wavelength, with temperatures tied to that of the first Mekal component, but with normalisations allowed to

vary. This broadened the line profile of the model to mimic the degraded resolution of the RGS for the extended emission line region. We then added a second, lower temperature, broadened Mekal component to the model. This resulted in another significant improvement in χ^2 , reproducing most of the emission lines well, with the second plasma component at a best fit temperature of ~ 0.2 keV, consistent with the temperature deduced from the O VII lines (Sect. 2.2). However, although χ^2 is good, the blend of Ne X with Fe XXI-XXIII at ~ 12.1 \AA is still underproduced by this model, and so a third, higher temperature, broadened Mekal plasma was added. This resulted in yet another significant improvement in the fit, to a final best $\chi^2/\nu = 803/980$, with a best fit temperature for the third Mekal component of $1.7^{+2.1}_{-0.5}$ keV. The model reproduces the spectrum well, as shown in Fig.4.

We have not attempted to derive elemental abundances for the soft X-ray emission line gas, because the abundance ratios are somewhat degenerate with the temperature structure of the gas. However, we have verified that our assumption of solar abundance is reasonable as follows. Fe and O are responsible for the strongest soft X-ray lines in M81, so the ratio of Fe to O will be the most important abundance ratio in terms of the resultant emission line spectrum, and the easiest to determine. We have therefore repeated the three-Mekal fit, once with the Fe abundance halved, and once with the Fe abundance doubled, but with the abundances of other elements (including O) fixed at the solar values (Anders & Grevesse 1989). We find that with the Fe abundance halved, the best fit is worse by $\Delta\chi^2 = 4$, while doubling the Fe abundance results in a best fit that is worse by $\Delta\chi^2 = 9$, with respect to the three-Mekal, solar-abundance fit in Table 2. This suggests that the thermal plasma in M81 has an Fe to O ratio reasonably close to solar.

3. Discussion

In Sect. 2.2 we showed that the soft X-ray emission lines in M81 come from a region which is extended in both the dispersion direction (evidenced by the excess width of the lines) and cross dispersion direction (see Fig.1) of the RGS. We also showed that the diagnostic OVII triplet is emitted by a low density plasma and is not powered by photoionization from the central AGN. Furthermore, in the previous section we showed that a 3 temperature thermal plasma model provides a good description of the emission line component of the M81 RGS spectrum in conjunction with absorbed power law emission from the nucleus. Two of the plasma components have well constrained temperatures of 0.18 ± 0.04 keV and 0.64 ± 0.04 keV, which are characteristic of the hot interstellar medium produced by supernova explosions; in this case we would expect these emission lines to come from a genuinely diffuse region (or regions) in the bulge of M81.

X-ray imaging studies, first using *ROSAT* (Roberts & Warwick 2000, Immler & Wang 2001) and later using *Chandra* (Tennant et al. 2001) have indeed found appar-

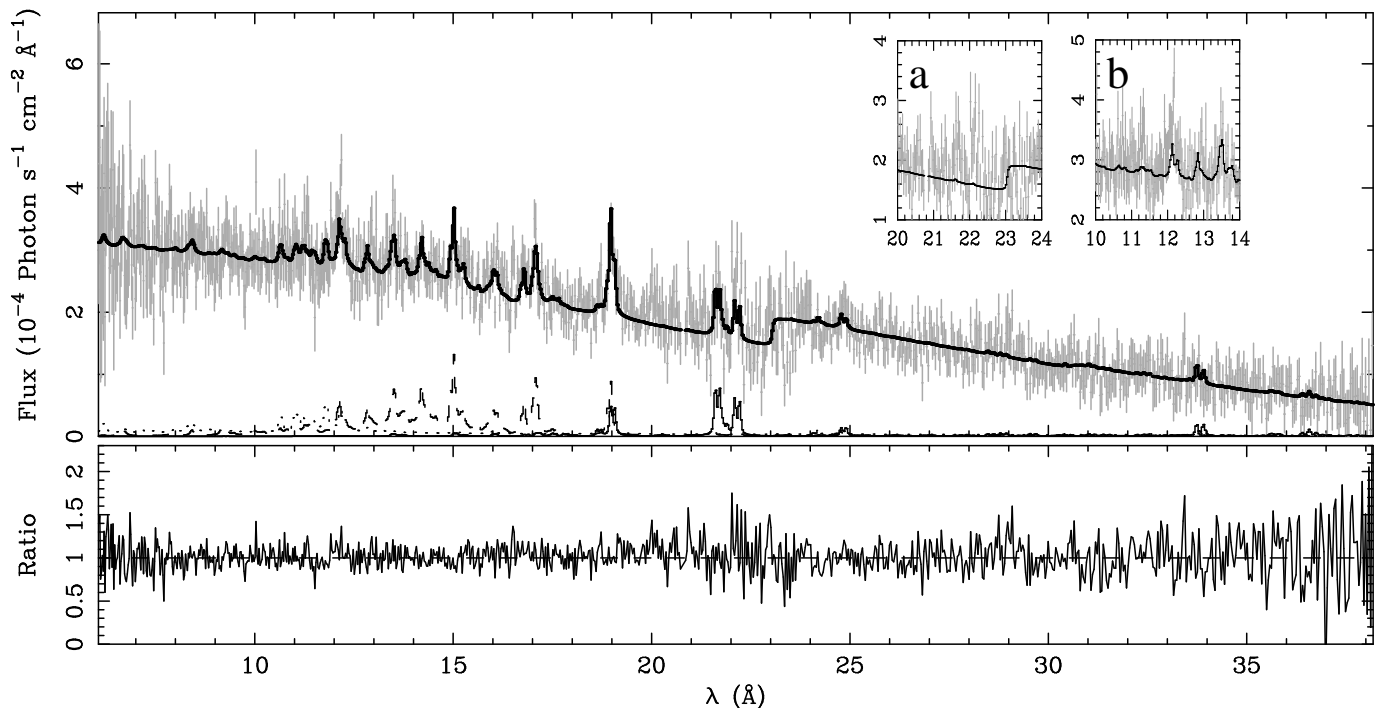


Fig. 4. Power law \times intrinsic neutral absorption + 3 Mekal model fit to the RGS spectrum. The top panel shows the data (grey points) and model (bold black line) while the bottom panel shows the data/model ratio. Also shown in the top panel is the contribution from the three different temperature thermal plasma components: 0.18 keV (thin solid line), 0.64 keV (dashed line) and 1.7 keV (dotted line). Inset a displays data and single-temperature Mekal model around the OVII triplet, showing that O VII lines are not reproduced by the single temperature model. Inset b shows data and two-temperature Mekal model around the Ne X / Fe XXI-XXIII blend, indicating that a third, higher-temperature model component is required to reproduce these lines.

ently diffuse emission associated with the bulge of M81. Furthermore, Immler & Wang (2001) extracted a PSPC spectrum of the M81 bulge using a 1 arc-minute radius source circle, including both the active nucleus and the diffuse emission. They found a good fit using an absorbed power law to represent the nucleus and a two temperature thermal plasma to represent the apparently diffuse emission. Their best fit plasma temperatures, 0.15 ± 0.02 keV and 0.63 ± 0.11 keV, are in extremely good agreement with the temperatures obtained from the RGS spectrum. However the spatial resolution of *ROSAT* (~ 5 arc-second for the HRI and ~ 20 arc-second for the PSPC) was such that the emission from a large population of weak point sources could easily be confused with genuinely diffuse emission.

The much higher resolution observation performed with *Chandra* provides a much more accurate determination of the truly diffuse emission from the nucleus. Tennant et al. (2001) found that of the bulge emission, even excluding the nucleus, 64% comes from the resolved point source population. The remaining unresolved bulge emission reported by Tennant et al. (2001) has a count-rate of 0.092 s^{-1} in the *Chandra* ACIS-S3 chip. The 0.18 keV and 0.64 keV thermal plasma components from our

best fit model in Table 1 would correspond to count-rates of 0.036 s^{-1} and 0.158 s^{-1} in the same chip. The lowest temperature component alone is unable to account for all the unresolved bulge emission, but the combination of the two exceeds it.

This implies that some of the emission associated with the 0.64 keV thermal plasma, and all of the emission associated with the highest of the three plasma temperatures ($1.7^{+2.1}_{-0.5}$ keV) must arise in part of the bulge population resolved by *Chandra*. We therefore propose low-mass X-ray binaries as the most likely origin of this higher temperature emission.

The line-of-sight velocity dispersion in the bulge of M81 is $165 \pm 10 \text{ km s}^{-1}$ (Prichet 1978, Pellet & Simien 1982), so the 0.2 keV plasma has similar energy per unit mass to the stellar component and is bound to the bulge. Using the cooling curves from Landini & Monsignori Fossi (1990) we find that the cooling time for the 0.2 keV component is $\sim 4 \times 10^7 / \sqrt{f}$ years where f is the filling factor of the gas. This is much shorter than the time since the last M81–M82 perigalactic passage ($\sim 5 \times 10^8$ years ago, Brouillet et al. 1991; Chandar et al. 2001) and hence the 0.2 keV gas, which has a mass of $10^6 / \sqrt{f} M_{\odot}$, cannot be a relic of a nuclear starburst induced by the passage of M82

Table 2. Spectral fitting of the whole M81 RGS spectrum. All models include Galactic absorption of $N_{\text{H}} = 4.16 \times 10^{20} \text{ cm}^{-2}$

(1) Model	(2) Γ or kT	(3) flux	(4) N_{H}	(5) χ^2/ν
PL	1.67 ± 0.02	105 ± 1		1289/993
PL \times N_{H}	2.06 ± 0.06	99.9 ± 3.8	4.8 ± 0.8	1085/992
PL \times N_{H} +Mek	1.94 ± 0.07 0.66 ± 0.04	95.8 ± 3.7 $4.3^{+0.9}_{-0.7}$	3.3 ± 0.8	876/990
PL \times N_{H} +Mek3	1.92 ± 0.07 0.64 ± 0.04	95.4 ± 3.7 $4.7^{+0.9}_{-0.7}$	3.1 ± 0.8	866/988
PL \times N_{H} +Mek3 +Mek3	1.93 ± 0.07 $0.20^{+0.04}_{-0.02}$ 0.66 ± 0.05	94.5 ± 3.8 1.5 ± 0.5 $4.2^{+0.8}_{-0.7}$	3.4 ± 0.8	821/984
PL \times N_{H} +Mek3 +Mek3 +Mek3	1.94 ± 0.06 0.18 ± 0.04 0.64 ± 0.04 $1.7^{+2.1}_{-0.5}$	$91.6^{+7.4}_{-4.4}$ $1.1^{+0.5}_{-0.4}$ $4.2^{+0.8}_{-0.9}$ $3.4^{+7.6}_{-2.2}$	3.4 ± 0.8	803/980

Explanation of columns:

1 PL = power law,

N_{H} = neutral absorber ('tbabs' model in XSPEC),

Mek = thermal plasma ('Mekal' model in XSPEC),

Mek3 = thermal plasma ('Mekal' model in XSPEC) with components shifted by $\pm 0.5\%$ in wavelength to mimic the broadening of the lines produced by the spatial extent of the emission region.

2 power law photon index or temperature of thermal plasma (keV)

3 flux of model component in the energy range 0.3-2.0 keV, in units of $10^{-13} \text{ erg cm}^{-2} \text{ s}^{-1}$ without Galactic absorption of $N_{\text{H}} = 4.16 \times 10^{20} \text{ cm}^{-2}$

4 intrinsic neutral column density (10^{20} cm^{-2}).

because the gas must have been replenished or reheated much more recently. The 0.64 keV component has a mass of $1.4 \times 10^6 / \sqrt{f} M_{\odot}$, and potentially has a much longer cooling time, $\sim 3 \times 10^5 / \sqrt{f}$ years, but it is too hot to be bound by the virial mass of the bulge. The sound crossing time for the bulge of M81 is less than 10^7 years, so the 0.64 keV gas must also be replenished or reheated on a timescale of a few $\times 10^7$ years.

The simulations of Shelton (1998) allow us to estimate the approximate supernova rate that would sustain the diffuse X-ray luminosity of the bulge of M81. The combined flux from our two lowest temperature thermal components, compared to the predicted *ROSAT* countrates from section 7.4 of Shelton (1998) corresponds to supernova rates of between $\sim 4 \times 10^{-3} \text{ year}^{-1}$ and $\sim 4 \times 10^{-2} \text{ year}^{-1}$, where the lower estimate comes from the predicted countrate in the lower energy R1 *ROSAT* band and the higher estimate comes from the predicted countrate in the

higher energy R4 *ROSAT* band. The flux in the *ROSAT* R4 band is dominated by the 0.64 keV plasma; if we assume that half of this emission is due to resolved sources then the R4-band estimate of the supernova rate is reduced to $\sim 2 \times 10^{-2} \text{ year}^{-1}$. If the supernova rate in the bulge of M81 is $\sim 4 \times 10^{-3} \text{ year}^{-1}$ or higher we expect there to be tens of supernova remnants within the bulge with ages $< 10^4$ years, although in the gas-poor environment of the bulge they may have very low X-ray luminosities. There are 41 sources detected by *Chandra* within the bulge of M81, of which $\sim 30\%$ have spectra which are softer than typical X-ray binaries (Tennant et al. 2001). The collective flux of these sources is sufficient to contribute significantly to the 0.64 keV plasma emission; further *Chandra* observations will be required to determine whether these sources are persistent and thus potential supernova remnants.

UV imaging carried out with the Hubble Space Telescope failed to reveal any individual massive stars in the bulge (Devereux et al. 1997), and this lack of a young, massive stellar population leaves only type 1a supernovae as the possible origin of the X-ray emitting gas. We obtain the canonical 'expected' rate for type 1a supernovae in M81 from table 8 of Van den Bergh & Tammann (1991). Assuming a distance of 3.6 Mpc, B magnitude of 7.31 after correction for Galactic extinction (de Vaucouleurs et al. 1991) and $H_0 = 75 \text{ km s}^{-1} \text{ Mpc}^{-1}$, we expect $\sim 6 \times 10^{-3}$ type 1a supernovae year^{-1} for the whole galaxy, consistent with the rate of supernovae required to support the diffuse X-ray emission.

The diffuse X-ray emission may well relate to the optical line emission which gives M81 its LINER classification. The bulge of M81 is bright in H α emission (Devereux et al. 1995, Greenwalt et al. 1998), and in the absence of young massive stars Devereux et al. (1997) conclude that the diffuse H α emission must be powered either by old post-AGB stars or by shocks, both of which are compatible with the observed UV surface brightness. If the diffuse X-ray emission is indeed produced by supernova remnants, then fast shocks must be propagating through the bulge.

There are three pieces of evidence that suggest shocks related to the X-ray emitting gas, rather than post-AGB stars, ionize the diffuse optical emission line gas. Firstly, the H α emission region has a similar spatial extent to the X-ray line emitting plasma, but it has an asymmetric, possibly spiral structure (Devereux et al. 1995, Greenwalt et al. 1998), and hence does not trace the underlying distribution of stars in the bulge, as might be expected if the gas is ionized by old post-AGB stars. Secondly, the ionized H α emitting gas shows complex, non-rotational motion of up to 200 km s^{-1} , as well as rotation at up to 300 km s^{-1} (Goat 1976). The non-rotational motion could be driven by the expansion of hot bubbles and suggests mechanical heating of the gas. Thirdly, the optical emission line ratios suggest that photoionization by hot stars is not the ionization mechanism in the bulge. For example, the [SII]/(H α + [NII]) ratio is much higher in the bulge of M81 than in any of the HII regions, (Greenawalt et

al. 1998), suggesting that photoionization by hot stars is not the ionization mechanism in the bulge. However shock heating, with shock velocities of a few hundred km s^{-1} , can result in large $[\text{S II}]/\text{H}\alpha$ ratios (Baum et al. 1992, Dopita & Sutherland 1995) as observed. Furthermore, the strength of $[\text{O III}] \lambda 5007$ observed in the central few hundred pc of M81 cannot be reproduced by photoionization from hot stars (Golev et al. 1996; Wang et al. 1997), but the $[\text{O III}]/\text{H}\beta$ ratio is similar to the predictions of the shock model of Dopita & Sutherland (1995) for shock velocities of 300 km s^{-1} . In this model, $[\text{O III}] \lambda 5007$ is emitted by gas which is photoionized by the shock-heated material. For a shock velocity of 300 km s^{-1} the shocked material has an electron temperature similar to the 0.2 keV plasma found in the RGS spectrum (Dopita & Sutherland 1996). This suggests that the optical line-emission is related to the soft X-ray line-emitting plasma, and that the ISM in the bulge of M81 is shock-heated, possibly by supernovae.

4. Conclusions

The *XMM-Newton* RGS soft X-ray spectrum of M81 shows emission lines from H-like and He-like N, O and Ne as well as Fe-L lines superimposed on a strong continuum from the nucleus. The excessive width of the emission lines in the dispersion direction, and their detection outside the nucleus in the cross dispersion direction implies that the emission lines originate in a region of a few arcminutes spatial extent, corresponding to a few kpc in M81. The OVII triplet line ratios suggest that photoionization is not the main ionization mechanism and that collisional processes must be important in producing the observed lines. The RGS spectrum can be fitted with a model consisting of an absorbed power law from the nucleus and a 3 temperature optically thin thermal plasma. Two of the thermal components have temperatures ($0.18 \pm 0.04 \text{ keV}$ and $0.64 \pm 0.04 \text{ keV}$) which are consistent with the hot interstellar medium produced by supernovae; the combined flux from these two components fully accounts for (in fact exceeds) the unresolved bulge emission seen with *Chandra*. The X-ray emission could be produced by type Ia supernova rates of $\sim 4 - 20 \times 10^{-3} \text{ year}^{-1}$, which is not unreasonable for M81. We propose that the shocks generated by the supernova remnants could also be responsible for the observed optical line emission in the bulge of M81. The third X-ray emitting thermal plasma component has a higher temperature ($1.7_{-0.5}^{+2.1} \text{ keV}$) and in order not to exceed the unresolved X-ray emission found with *Chandra* we propose X-ray binaries in the bulge of M81 as a likely origin of this emission, as well as \sim half of the 0.64 keV emission.

References

Anders E. & Grevesse N., 1989, *Geochimica et Cosmochimica Acta*, 53, 197
 Baum S.A., Heckman T.M. & van Breugel W., 1992, *ApJ*, 389, 208

Brouillet N., Baudry A., Combes F., Kaufman M. & Bash F., 1991, *A&A*, 242, 35
 Chandar R., Tsvetanov Z. & Ford H.C., 2001, *ApJ*, 122, 1342
 Devereux N.A., Jacoby G. & Ciardullo R., 1995, *AJ*, 110, 1115
 Devereux N., Ford H. & Jacoby G., 1997, *ApJ*, 481, L71
 Dickey J.M. & Lockman F.J., 1990, *Ann. Rev. Ast. Astr.*, 28, 215
 Dopita M.A. & Sutherland R.S., 1995, *ApJ*, 455, 468
 Dopita M.A. & Sutherland R.S., 1996, *ApJS*, 102, 161
 Elvis M. & van Speybroeck L., 1982, *ApJ*, 257, L51
 Fabbiano G., 1988, *ApJ*, 325, 544
 Goad J.W., 1976, *ApJS*, 32, 89
 Greenawalt B., Walterbos R.A.M., Thilker D. & Hoopes C.G., 1998, *ApJ*, 506, 135
 den Herder J.W., et al., 2001, *A&A*, 365, L7
 Golev V., Yankulova I., & Bonev T., 1996, *MNRAS*, 280, 29
 Heckman T.M., 1980, *A&A*, 87, 152
 Ho L.C., Filippenko A.V. & Sargent W.L.W., 1997, *ApJ*, 487, 568
 Immler S. & Wang Q.D., 2001, *ApJ*, 554, 202
 Ishisaki Y., et al., 1996, *PASJ*, 48, 237
 Landini M., & Monsignori Fossi B.C., 1990, *A&AS*, 82, 229
 Pellegrini S., et al., 2000, *A&A*, 353, 447
 Pellet A., & Simien F., 1982, *A&A*, 106, 214
 Petre R., Mushotzky R.F., Serlemitsos P.J., Jahoda K. & Marshall F.E., 1993, *ApJ*, 418, 644
 Porquet D. & Dubau J., 2000, *A&A Supp*, 143, 495
 Porquet D., Mewe R., Dubau J., Raassen A.J.J. & Kaastra J.S., 2001, *A&A*, 376, 1113
 Pritchett C., 1978, *ApJ*, 221, 507
 Roberts T.P. & Warwick R.S., 2000, *MNRAS* 315, 98
 Shelton R.L., 1998, *ApJ*, 504, 785
 Tennant A.F., Wu K., Ghosh K.K., Kolodziejczak J.J. & Schwartz D.A., 2001, *ApJ*, 549, L43
 van den Bergh S. & Tammann G.A., 1991, *Annu. Rev. Astron. Astrophys.*, 29, 363
 de Vaucouleurs G., et al., 1991, 'Third Reference Catalogue of Bright Galaxies' Springer-Verlag
 Wang J., Heckman T.M. & Lehnert M.D., 1997, *ApJ*, 491, 114
 Wilms J., Allen A. & McCray R., 2000, *ApJ*, 542, 914